

Published in final edited form as:

*J Control Release*. 2011 February 10; 149(3): 242–249. doi:10.1016/j.jconrel.2010.10.033.

## Separable Arrowhead Microneedles

Leonard Y. Chu<sup>1</sup> and Mark R. Prausnitz<sup>1,2,\*</sup>

<sup>1</sup>Wallace Coulter Department of Biomedical Engineering, Georgia Institute of Technology, Atlanta, GA 30332, USA

<sup>2</sup>School of Chemical and Biomolecular Engineering, Georgia Institute of Technology, Atlanta, GA 30332, USA

### Abstract

Hypodermic needles cause pain and bleeding, produce biohazardous sharp waste and require trained personnel. To address these issues, we introduce separable arrowhead microneedles that rapidly and painlessly deliver drugs and vaccines to the skin. These needles are featured by micron-size sharp tips mounted on blunt shafts. Upon insertion in the skin, the sharp-tipped polymer arrowheads encapsulating drug separate from their metal shafts and remain embedded in the skin for subsequent dissolution and drug release. The blunt metal shafts can then be discarded. Due to rapid separation of the arrowhead tips from the shafts within seconds, administration using arrowhead microneedles can be carried out rapidly, while drug release kinetics can be independently controlled based on separable arrowhead formulation. Thus, drug and vaccine delivery using arrowhead microneedles are designed to offer a quick, convenient, safe and potentially self-administered method of drug delivery as an alternative to hypodermic needles.

### Keywords

Drug delivery; Microneedle; Hypodermic injection; Microfabrication; Skin; Transdermal drug delivery

## 1 Introduction

Currently, biopharmaceuticals are delivered almost exclusively by hypodermic needles, with over 16 billion injections given worldwide each year [1]. However, injection using hypodermic needles is not well-accepted by patients due to pain, bleeding and fear of needles. Needle phobia is common and has been shown to reduce the willingness of patients to receive treatment or vaccination [2,3]. In addition, unsafe injection practices, such as needle sharing and reuse, account for more than 50% of all injections in developing countries [4]. As a result of unsafe injections, transmission of blood-borne pathogens including hepatitis B, hepatitis C and HIV cause more than 1.3 million deaths and cost more than US\$535 million per year in direct medical expenditures [5]. Finally, proper handling

© 2010 Elsevier B.V. All rights reserved

\*Address editorial correspondence to Prof. Mark R. Prausnitz School of Chemical and Biomolecular Engineering Georgia Institute of Technology 311 Ferst Drive Atlanta, GA 30332-0100 USA Ph: +1 (404) 894-5135 Fax: +1 (404) 894-2291 prausnitz@gatech.edu.

**Publisher's Disclaimer:** This is a PDF file of an unedited manuscript that has been accepted for publication. As a service to our customers we are providing this early version of the manuscript. The manuscript will undergo copyediting, typesetting, and review of the resulting proof before it is published in its final citable form. Please note that during the production process errors may be discovered which could affect the content, and all legal disclaimers that apply to the journal pertain.

and disposal of hypodermic needle waste adds additional costs and is often done improperly [6].

For these and other reasons, there have been intensive efforts to develop alternate delivery methods to replace hypodermic needles. For example, conventional transdermal patches can administer a number of different low-molecular weight, low-dose drugs across the skin in a non-invasive manner [7]. Novel methods, such as ultrasound [8], skin abrasion [9,10] and thermal ablation [7,11] have been used to increase skin permeability and thereby enable delivery of macromolecules, such as proteins and vaccines. However, these methods generally require a two-step process that involves skin permeabilization followed by drug patch application, which introduces opportunity for procedural mistakes and requires patient training. Moreover, these methods require patients to wear a patch over a long time as drug slowly diffuses from the patch and into the skin.

As a balance between invasive hypodermic needles and non-invasive transdermal patches, we and others have proposed the use of microneedles as a minimally invasive method that seeks to capture the advantages of the needle and the patch, while avoiding their shortcomings. Solid metal microneedles coated with drug have been used to administer parathyroid hormone [12], influenza vaccine [13] and other compounds. Using this approach, microneedles can be easily and painlessly inserted into the skin [14,15]. Dissolution of the drug coating in skin takes a number of minutes, after which the metal microneedles are discarded as biohazardous sharp waste.

Dissolving microneedles represent an improvement over coated microneedles because they eliminate biohazardous waste. Using this technology, drug is encapsulated within a microneedle made of a safe, water-soluble materials, which fully dissolve in the skin, leaving only the patch backing to be discarded [16–19]. However, dissolving microneedles require many minutes to dissolve and typically have difficulty being fully inserted into skin due to the wider needle geometry needed to give these needles sufficient mechanical strength [19,20].

In this study, we introduce separable arrowhead microneedles, which are designed to overcome these limitations by combining the mechanical strength of metal microneedles with the elimination of biohazardous sharp waste enabled by dissolving microneedles and adding the capability to administer drug within seconds after patch application. Separable arrowhead microneedles mount a water soluble, pyramid-shaped “arrowhead” encapsulating drug onto a metal shaft. The shaft serves as a mechanically strong spacer that overcomes skin deformation during microneedle insertion to fully embed the drug-loaded arrowhead in the skin. The arrowheads can be designed to separate from the shafts within seconds. After separation, the blunt shafts can be safely discarded, possibly without special handling. In this way, separable arrowhead microneedles could enable simple, rapid self-administration of drugs that would otherwise require hypodermic injection.

## 2 Materials and Methods

### 2.1 Microneedle Fabrication

**2.1.1 Microneedle Mold**—A polydimethylsiloxane (PDMS, Sylgard 184, Dow Corning, Midland, MI) mold was fabricated using photolithography and molding techniques to generate a  $10 \times 10$  array of pyramidal microneedle cavities used to form the microneedle arrowheads [21]. Each cavity was  $600 \mu\text{m}$  deep with a  $300 \mu\text{m} \times 300 \mu\text{m}$  square base and tapered to a tip of  $10 \mu\text{m}$  radius. Center-to-center spacing between cavities was  $640 \mu\text{m}$ . A polylactic acid (PLA) microneedle master structure was made by casting molten PLA (L-PLA, 1.0 dL/g; Birmingham Polymer, Pelham, AL) onto the PDMS mold under vacuum at

−91 kPa for 1 h at 195°C. PDMS mold replicates were made by curing PDMS on top of the PLA master structure at 37°C overnight.

**2.1.2 Fabrication of Microneedle Shafts and Backing**—A 125 μm-thick stainless steel sheet (McMaster-Carr, Atlanta, GA) was cut using an infrared laser (Resonetics Maestro, Nashua, NH) at a cutting velocity of 1 mm/s with one pass, 20% attenuation of laser energy, and air purge at a constant pressure of 140 kPa based on AutoCAD (Autodesk, Cupertino, CA) drawings. Laser-patterned shafts were cut into the metal sheet with widths of 320 μm and lengths of 400–1000 μm. Center-to-center spacing between needles was 640 μm. Array size varied from 5 × 5 to 5 × 10 for a total of 25 to 50 microneedles. To define the extent of the overlap between the shaft and the arrowhead, rectangular stoppers were patterned on the periphery of the shaft array with a width of 300 μm and a length approximately 100 μm shorter than the shaft. The shafts and the stoppers were then bent 90° out-of-plane using a razor blade while viewing under a stereomicroscope. The processed metal pieces with bent shafts were electropolished using electropolishing solution (E972, ESMA Inc., South Holland, IL) in an E399 electropolisher (ESMA Inc.) for 15 min at 2 A at 45°C. The electropolished metal pieces were briefly rinsed in 30% nitric acid solution, cleaned with DI water and blow-dried with nitrogen gas.

**2.1.3 Microneedle Matrix and Formulation Preparation**—Different polymer matrix solutions were prepared to encapsulate sulforhodamine B (Molecular Probes, Eugene, OR) or inactivated influenza virus (A/Puerto Rico/8/34, Emory Vaccine Center, Atlanta, GA). To encapsulate sulforhodamine B, a polymer blend consisting of polyvinyl alcohol (PVA) (MW 2000 Da, ACROS Organics, Geel, Belgium) and polyvinylpyrrolidone (PVP) (BASF, K17, MW ~10000 Da, Aktiengesellschaft, Ludwigshafen, Germany) (mass ratio 1:1) was prepared. Two grams of PVA was dispersed in 3 ml of DI water at 25°C and then heated to 90°C for 1 h to solubilize. An additional 2 g of PVP was added and mixed homogeneously with the PVA solution. The polymer blend was incubated at 60°C for 5–6 h and cooled to room temperature before use. To encapsulate inactivated influenza virus, a blend of PVA and sucrose (Sigma-Aldrich, St Louis, MO) (mass ratio 1:1) was prepared. Similarly, 2 g of sucrose was dissolved in the PVA solution and mixed homogeneously at 60°C and cooled to 25°C before use. All excipients, i.e., PVA, PVP, and sucrose, are commonly used pharmaceutical excipients with an excellent safety record in widespread clinical use.

**2.1.4 Drug Loading and Polymer Blend Casting**—To fabricate microneedles with water-soluble arrowheads, drug encapsulation was accomplished by a two-step process in which the drug/vaccine solution was first loaded into the cavities of the mold followed by casting of the designated polymer matrix solution [20]. A volume of 100 μl of sulforhodamine B (5 mg/ml) or inactivated influenza virus (0.5 mg/ml) solution was transferred onto the PDMS mold and vacuumed at −91 kPa for 3 min. Residual drug/vaccine solution on the mold surface was removed by pipetting and saved for later use, leaving the drug/vaccine solution only in the mold cavities. The drug/vaccine solution loaded in the mold cavities was then dried under centrifugation at 3200 × g at room temperature for 3 min. Immediately after drying, the designated polymer matrix solution was cast onto the mold under vacuum at −91 kPa for 3 min, cleaned from the mold surface, and then centrifuged again at 3200 × g at room temperature for 5 min.

To fabricate microneedles with biodegradable arrowheads, 10 mg sulforhodamine B was pre-mixed with 100 mg molten poly(DL-lactide-co-glycolide) (PLGA 50:50, inherent viscosity 0.55–0.75, Birmingham Polymer) to form a molten polymer matrix containing sulforhodamine B. The molten PLGA with sulforhodamine B was vacuumed at −91 kPa for 10 min at 195°C. While the mold still remained hot, the residual molten PLGA with sulforhodamine B on the mold surface was scraped off using a glass slide.

**2.1.5 Shaft Alignment and Drying**—To make a complete arrowhead microneedle patch, a microneedle shaft array was aligned manually to the mold cavities under a stereomicroscope (Olympus SZX16, Pittsburgh, PA). Gentle force was applied onto the metal backing against the mold until the stoppers located along the periphery of the shaft array hit the mold surface. This embedded the microneedle shafts between 100  $\mu\text{m}$  and 200  $\mu\text{m}$  into the base of the arrowheads. PVA/PVP microneedles encapsulating sulforhodamine B were dried at room temperature overnight, whereas PVA/sucrose microneedles encapsulating inactivated influenza virus were freeze-dried (VirTis Wizard 2.0 freeze dryer, Gardiner, NY) using the following program: the samples were frozen at  $-40^{\circ}\text{C}$  for 1 h, and then vacuumed at  $-101$  kPa at  $-40^{\circ}\text{C}$  for 10 h. While the pressure was kept constant at  $-101$  kPa, the temperature was gradually ramped up to  $0^{\circ}\text{C}$  for 1 h,  $20^{\circ}\text{C}$  for 1 h and  $25^{\circ}\text{C}$  for another 10 h. PLGA microneedles were simply cooled to room temperature without drying.

After drying/solidification, the arrowheads connected to the shaft arrays were removed from the mold to yield complete arrowhead microneedle patches. Prior to microneedle insertion into the skin, the stoppers located along the periphery of the shaft array were bent onto the base of the array so that they would not interfere with subsequent skin insertion.

## 2.2 In Vitro Test

**2.2.1 Microneedle Insertion and Evaluation**—Prior to microneedle insertion, porcine cadaver skin (Pel-Freez, Rogers, AR) was processed by removing hair using a razor (Dynarex, Orangeburg, NY) and subcutaneous fat using a scalpel with approval from the Georgia Tech IACUC. While holding the skin under mild tension using two fingers, microneedles were manually pressed against the skin from a distance of approximately 1 cm. To enable arrowhead separation by dissolution, the needles were left inserted in the skin for a designated time. To enable arrowhead separation by mechanical separation, manual vibration was applied to the needles against the skin immediately after insertion for  $< 1$  s.

Human cadaver skin was obtained from the Emory University School of Medicine (Atlanta, GA) with approval from the Georgia Tech IRB. To prepare human cadaver skin for insertion test, subcutaneous fat was removed by a scalpel. To evaluate the ability of arrowhead microneedles to pierce into human cadaver skin before and after use, three versions of needles were tested: intact arrowhead microneedles; blunt metal shafts without arrowheads; and sharp metal structures of the same length as the blunt microneedle shafts, but tapered to a sharp tip (i.e., similar to metal microneedles used in other studies [12,13,15,22]). Each needle type was applied to the human cadaver skin as described above, after which the skin was stained with tissue marking dye for 5 min and then cleaned from the skin surface using paper towels and alcohol swabs. All images of the microneedles and application sites on the skin were taken using a stereomicroscope (Olympus SZX16) with a digital camera (Olympus DP71).

**2.2.2 Imaging and Histology**—Microneedle insertion sites were excised from bulk skin using a scalpel. Each isolated skin piece was embedded in Optimum Cutting Temperature (OCT) media (Tissue-Tek, Torrance, CA) in a cryostat mold. The sample was fixed by freezing the OCT sample on dry ice. Frozen OCT samples were sliced into 12- $\mu\text{m}$  thick sections using a cryostat (Cryo-star HM 560MV, Microm, Waldorf, Germany) and placed on glass slides. Fluorescence images were taken (Nikon E600, Tokyo, Japan) prior to staining. The same skin sections were then subject to hematoxylin and eosin (H&E) staining using an automated staining machine (Leica Autostainer XL, Nussloch, Germany). A few drops of cytoaseal 60 (low viscosity, Richard-Allan Scientific, Kalamazoo, MI) were applied onto the stained skin sections. The samples were then covered with glass cover slips and

dried in a fume hood over night. Images of the stained skin sections were taken under bright field using the Nikon microscope.

## 3 Results

### 3.1 Arrowhead Microneedle Fabrication

In this study, microneedles were designed to achieve three goals: (i) deliver the entire intended dose by completely embedding the microneedle tips within the skin, (ii) require only a short administration time of seconds, and (iii) generate no biohazardous sharp waste. To accomplish these goals, we developed arrowhead microneedles consisting of a dissolvable or biodegradable arrowhead encapsulating drug or vaccine mounted on a mechanically strong shaft to facilitate complete insertion into the skin.

Arrowhead microneedle patches were fabricated by separately preparing arrowheads encapsulating drug/vaccine and arrays of metal shafts, which were then combined to create arrowhead microneedle patches. To prepare the arrowheads, a drug solution was first cast onto a PDMS micromold (Fig. 1A). Residual drug on the mold surface was then removed and saved for future use, leaving drug solution filling only the mold cavities (Fig. 1B). After drying the drug within the mold cavities (Fig. 1C), we performed a second mold-filling step by casting drug-free aqueous polymer matrix solution into the mold cavities, which blended with the dried drug film within the mold cavities (Figs. 1D – 1E).

Metal shafts were laser cut, bent out-of-plane, electropolished, and then aligned and dipped into the mold cavities filled with polymer matrix solution with drug (Fig. 1F). The stoppers located along the periphery of the metal shaft array limited the depth of microneedle shaft penetration into the microcavities, which defined the degree of overlap between the shaft and the arrowhead (Fig. 1F), which was adjusted to be between 100  $\mu\text{m}$  and 200  $\mu\text{m}$ . After drying, the arrowhead microneedle patch was removed from the mold (Fig. 1G) and the stoppers were manually bent to the plane of the backing (Fig. 1H).

Using this approach, we fabricated arrowhead microneedles of different geometries and with different numbers of needles per array encapsulating different types of molecules. For example, a  $5 \times 5$  array of arrowhead microneedles encapsulating sulforhodamine B is shown in Fig. 2A. Each needle consists of a 600  $\mu\text{m}$ -long PVP/PVA arrowhead capped onto a metal shaft with an exposed length of 600  $\mu\text{m}$  and a 100  $\mu\text{m}$  overlap. The needle shaft's front dimension was made wider (i.e., 320  $\mu\text{m}$ , Fig. 2A1) to offset the mechanically weaker and thinner side of the shaft determined by the metal sheet thickness (125  $\mu\text{m}$ ; Fig. 2A2).

A larger array ( $5 \times 10$ ) containing 50 needles encapsulating inactivated influenza virus is shown in Fig. 2B. Each needle is capped with a 600  $\mu\text{m}$ -long PVP/sucrose arrowhead mounted on a metal shaft with an exposed length of 700  $\mu\text{m}$  and a 150  $\mu\text{m}$  overlap. The needles encapsulating influenza virus appear colorless (Fig. 2B1), whereas the encapsulation of sulforhodamine B appears pink.

### 3.2 Depth of Arrowhead Delivery Into Skin

The separable arrowhead microneedle design is hypothesized to enable complete insertion of drug-loaded arrowheads in the skin. This contrasts with conventional dissolving microneedles, in which a sometimes large fraction of the microneedle remains outside the skin due largely to skin deformation during microneedle application [19,20]. To test this hypothesis, we manually applied a separable arrowhead microneedle patch encapsulating sulforhodamine B to porcine cadaver skin for 3 min and then assessed efficiency of delivery. As shown under brightfield (Fig. 3A1) and fluorescence (Fig. 3A2) optics, the sulforhodamine B was delivered at each of the 25 microneedle insertion sites under the

patch. To determine if the dye had truly been delivered into the skin, as opposed to the skin surface, we tape stripped the skin surface up to 3 times at those insertion sites, but found almost no sulforhodamine removed by the tape (data not shown). This indicates that essentially all of the sulforhodamine had been delivered inside the skin because the arrowheads were fully inserted into the skin.

To better image the depth of arrowheads in the skin, we also examined microneedle insertion sites histologically. Figure 3B1 shows that the arrowheads (600  $\mu\text{m}$  long) were completely inserted into the skin, creating approximately 600  $\mu\text{m}$  deep cavities in the approximate shape of the arrowheads. Local release of encapsulated sulforhodamine from the dissolved arrowheads is shown by fluorescence imaging in Fig. 3B2.

In the above analysis, arrowheads were mounted on top of 600  $\mu\text{m}$  long shafts. To determine the effect of shaft length on insertion depth, we investigated three different shaft spacer lengths – 300, 600 and 900  $\mu\text{m}$  (Figs. 4A, 4B, and 4C, respectively) – capped with a 600  $\mu\text{m}$  arrowhead. Arrowheads mounted on the shortest shaft generated an approximately 300  $\mu\text{m}$  deep cavity in the skin, which indicated incomplete insertion of the 600  $\mu\text{m}$  arrowhead (Figs. 4A1 and 4A2). Consistent with Fig. 3, the 600  $\mu\text{m}$ -long shafts inserted arrowheads approximately 600  $\mu\text{m}$  deep (Figs. 4B1 and 4B2), while the 900  $\mu\text{m}$ -long shafts inserted about 900  $\mu\text{m}$  deep (Figs. 4C1 and 4C2), both of which were deep enough to embed the arrowheads completely in the skin.

In each case, the depth of insertion into the skin was approximately 600  $\mu\text{m}$  less than the length of the arrowhead microneedle (e.g., the shortest microneedle had a 300  $\mu\text{m}$  shaft plus a 600  $\mu\text{m}$  arrowhead for a total length of 900  $\mu\text{m}$ , but only inserted to a depth of 300  $\mu\text{m}$ ). This indicates significant skin deflection under the conditions used in this study, which is why such long microneedle shafts were needed. Use of sharper arrowhead tips, skin with less toughness than pig skin, and further stretching of the skin would all reduce skin deflection during insertion and thereby enable arrowhead microneedles with shorter shafts to be effective.

### 3.3 Kinetics of Arrowhead Separation In the Skin

Separable microneedles are also hypothesized to enable rapid delivery to the skin (i.e., within seconds), which would simplify administration of a drug or vaccine by medical personnel or patients themselves. To achieve rapid separation of arrowheads from microneedle shafts, we formulated arrowheads with highly water-soluble excipients, such as PVP and sucrose. In addition, complete insertion of the arrowheads into the skin further expedited rapid arrowhead separation and dissolution by fully contacting them with skin's interstitial fluid.

We evaluated the kinetics of arrowhead separation by two different mechanisms. The first mechanism involves separation due to dissolution of the arrowhead by skin's interstitial fluid, which is limited by the rate of water diffusion into the arrowhead. The rate and extent of arrowhead separation were determined by measuring the amount of sulforhodamine lost from the microneedles and delivered into the skin. Within 5 s, almost 70% of the 9  $\mu\text{g}$  sulforhodamine encapsulated in the arrowheads was delivered (Fig. 5A). Within 60 s, approximately 90% was delivered.

To achieve still faster separation, the second mechanism relied on mechanical separation of the arrowheads from their shafts. Upon insertion, a gentle vibration was applied manually to the microneedle patch for < 1 s while pressed against the skin. Removal of the microneedle patch after just 1 s enabled delivery of more than 80% of the 9  $\mu\text{g}$  sulforhodamine (Fig 5B). Leaving the needles inserted in the skin for 5 s increased delivery efficiency to 90%. These

results suggest that arrowhead microneedles enable almost complete separation of the arrowhead within seconds of application to the skin.

### 3.4 Arrowhead Microneedles For Controlled Release

Although arrowhead separation can be achieved rapidly, in some cases it may be useful to release the drug from embedded arrowheads more slowly. To address this scenario, microneedles were prepared with arrowheads made of PLGA encapsulating sulforhodamine (Fig. 6A). After insertion and mechanical vibration, these PLGA arrowheads were deposited in the skin within 3 s for subsequent slow release without the need for extended patch wearing time (Fig. 6B).

### 3.5 Safety Evaluation of Microneedles After Use

Our final hypothesis is that separable arrowhead microneedles do not generate biohazardous sharp waste. To assess this, we first inserted an array of arrowhead microneedles containing sulforhodamine B (Fig. 7A) into human cadaver skin. These needles all penetrated deeply into the skin, as shown by the 50 red sulforhodamine B marks on the skin (Fig. 7A1). Next, we pressed blunt metal shafts without arrowheads (Fig. 7B) to the skin, but did not observe staining of the skin surface as an indication of perforation at the shaft application sites after applying black tissue marking dye (Fig. 7B1). However, the presence of lightly stained marks on the skin could be due to the difficulty of removing the residual dye stuck in the hair follicles, superficial skin scratches and excessive inelastic skin deformation generated by pressing the shafts against the skin. Finally, as a positive control, we sharpened the blunt shafts used for arrowhead microneedles (Fig. 7C) and applied them to the skin, which perforated the skin, as indicated by a clearly evident array of dots from the tissue marking dye (Fig. 7C1). These data demonstrate that the residual microneedle shafts from arrowhead microneedles are too blunt to easily pierce skin and therefore could be disposed of as non-sharp waste. Additional safety studies and device optimization are needed.

## 4 Discussion

Currently, administration of biopharmaceuticals and vaccines relies heavily on injection using hypodermic needles. This method of delivery generates pain, causes bleeding and generates patient apprehension [2,3,23]. Hypodermic needles also pose the risk of needle-stick injury and potential of needle reuse [24]. After administration, the needles become biohazardous sharp waste and must be disposed of properly.

Previous studies have proposed microneedles as an alternative delivery method to address limitations of hypodermic injection [25–27]. Previous microneedle designs have reduced or eliminated pain and bleeding [28,29] and dissolving microneedles have also eliminated needle re-use and biohazardous sharp waste disposal [16–19]. However, no previous microneedle design has been able to (i) deliver the entire intended dose by completely embedding the microneedle tips within the skin, (ii) require only a short administration time of seconds, and (iii) generate no biohazardous sharp waste. In this study, separable arrowhead microneedles were designed, fabricated and evaluated to achieve these three goals, which are critical to simple, safe, convenient and effective use for drug delivery. Featured by sharp arrowheads mounted on blunt shafts, this microneedle patch can insert drug-loaded arrowheads completely into the skin for efficient drug delivery. The arrowheads can either be dissolved or mechanically separated from the patch within seconds, leaving behind blunt shafts that can be disposed of safely.

#### 4.1 Complete Arrowhead Delivery Into Skin

Conventional microneedles coated with or encapsulating drugs must be inserted into the skin deep enough that the drug portion is fully embedded. The amount of drug delivered into the skin (i.e., bioavailability) is largely determined by the depth of microneedle penetration [20]. Coated metal microneedles can often be inserted fully into the skin, because of their slender profile enabled by the inherent mechanical strength of many metals [22,29]. However, metal microneedles produce biohazardous sharp waste.

Dissolving microneedles eliminate the sharp waste, but typically have difficulty being inserted fully into the skin [19,20]. This is because the mechanical weakness of water-soluble excipients used to make the microneedle matrix generally requires dissolving microneedles to have a wider needle base to increase mechanical strength and thereby prevent microneedle failure during insertion into skin. For this reason, dissolving microneedles usually cannot be inserted fully into the skin due to the impediment of the wider base and skin deformation. This means that (i) only a fraction of the encapsulated drug dose is delivered, (ii) microneedles must be left on the skin for longer times (e.g., many minutes) to enable dissolution of the portion of the microneedle outside the skin or (iii) drug can only be encapsulated within the tip of the microneedles, which significantly reduces drug dose per microneedle.

Separable arrowhead microneedles introduced in this study solve the issue of incomplete microneedle insertion by overcoming skin deformation by, in effect, mounting dissolving microneedles in the form of arrowheads on top of strong metal shafts. The shafts serve as both mechanical supports for insertion and spacers for skin deformation. Spacer length in this study was quite long (i.e. 600  $\mu\text{m}$ ), in order to overcome the tough and deformable pig skin excised from the body (Fig. 4). We expect that insertion into human skin under tension in the body in vivo will require a shorter spacer, given the reduced skin deformation under tension. In initial animal studies in vivo, arrowhead microneedles have been reliably inserted and separated in the skin of mice and guinea pigs (data not shown).

#### 4.2 Rapid Arrowhead Separation In the Skin

Administration time is an important consideration, especially when the target patient population is large and medical personnel are under time constraints [30]. Conventional transdermal patches require long hours of wearing time due to slow diffusion of drug across the skin barrier, which necessitates either extended patient interaction with a caregiver or reliance on patients to remove the patch after the right amount of time. Literature on dissolving microneedles has reported delivery times from minutes up to an hour for complete needle dissolution [16,18,19]. Studies on coated microneedles required patch wearing time up to 15 min [13,22] but needle application time as short as 1 min has been reported [29].

In our study, arrowheads were shown to separate in skin within 1 s and administer over 80% of encapsulated compounds (Fig. 5). Thus, the time required to administer drug using arrowhead microneedles can be comparable to hypodermic needles. This rapid administration is especially favorable in clinical practice, for example, when hospital traffic is busy or when conducting a mass vaccination campaign, or for self-administration, where patients may not properly follow instructions to leave a microneedle patch in place for a specified time. In this study, microneedle insertion and, in some cases, vibration on the skin surface, were carried out by expert research personnel. When used by untrained patients or caregivers, a simple patch applicator may be needed to provide the appropriate insertion force and possible vibration.



### 4.3 Microneedle Safety After Use

Biohazardous sharp waste continues to pose burdens on public health, as well as the environment. Separable arrowhead microneedles address this problem by using dissolvable or biodegradable sharp-tipped arrowheads. The choice of polymers for microneedles is limited to those that are mechanically robust for skin insertion, biocompatible, capable of dissolution in the skin, and provide a stable matrix for encapsulated drugs. The choice of drugs is limited to those of low dose (< 1 mg) and of low dermal irritancy/sensitization potential. After administration, these arrowheads become embedded within the skin for subsequent elimination from the body. Without sharp-tipped arrowheads, microneedle shafts cannot easily penetrate into the skin, which may permit safe disposal of used microneedle patches after arrowhead separation without the risk of needle-stick injury or the need for biohazardous sharp waste disposal systems.

### 4.4 Self-administration of Microneedles

Microneedles offer the promise of enabling patients to self-administer biopharmaceuticals and other drugs otherwise requiring hypodermic injection with the simplicity of a transdermal patch-like device. Separable arrowhead microneedles may provide the enabling design of microneedles that can realize this promise. This technology maintains the efficient and rapid administration associated with hypodermic injection, but eliminates the pain, bleeding, medical training and biohazardous sharp waste typically associated with needles. We envision patients purchasing microneedle patches at the pharmacy and self-administering them at home without special training. Patients should not have to worry about patch wearing time or premature patch removal when administering medication using separable arrowhead microneedles. After administration, the microneedle patch can be discarded, potentially in the conventional residential trash stream.

We also expect that the cost of separate arrowhead microneedle patches will be similar to that of other parenteral pharmaceuticals. Arrowhead microneedles consist of two parts: metal shaft and polymer arrowhead. The metal shaft array can be mass manufactured probably for less than \$0.01 per device. The arrowheads are molded onto the shafts using a simple process that is likely to have similar cost to conventional pharmaceutical lyophilization processes. Therefore, we believe that the system is economically viable with similar cost as lyophilized parenteral products. Because the materials costs are trivial, the primary cost of the microneedle patch is expected to be associated with its aseptic manufacturing, as well as the cost of the drug itself. These are the same cost drivers associated with other sterile pharmaceutical products requiring aseptic processing.

## 5 Conclusion

This study introduces separable arrowhead microneedles for rapid cutaneous delivery of drugs and vaccines. The novel design enables rapid and efficient delivery of drugs into the skin and does not generate biohazardous sharp waste. These microneedles include an arrowhead made of water-soluble excipients encapsulating the drug which is mounted on top of a strong metal shaft. Upon insertion into skin, the arrowhead is released in the skin on a time scale of seconds by either a rapid dissolution process or a still-faster method involving brief manual vibration. After arrowhead separation, the needles become dull and cannot easily be reused. We envision separable arrowhead microneedles as a quick, convenient, safe and potentially self-administered method of drug delivery as an alternative to hypodermic needles.

## Acknowledgments

We thank Dr. Seong-O Choi for providing the pyramidal microneedle master structure and we thank Dr. Mark Allen for use of his laser microfabrication facilities. This work was supported in part by the National Institutes of Health and carried out in the Center for Drug Design, Development and Delivery and the Institute for Bioengineering and Bioscience at the Georgia Institute of Technology. LYC carried out the experiments. LYC and MRP designed the studies and wrote the manuscript. MRP serves as a consultant and is an inventor on patents licensed to companies developing microneedle-based products. This possible conflict of interest has been disclosed and is being managed by Georgia Tech and Emory University.

## References

- [1]. Hutin YJF, Hauri AM, Armstrong GL. Use of injections in healthcare settings worldwide, 2000: literature review and regional estimates. *BMJ* 2003;327:1–5. [PubMed: 12842922]
- [2]. Hamilton JG. Needle phobia: A neglected diagnosis. *J. Fam. Pract* 1995;41:169–175. [PubMed: 7636457]
- [3]. Nir Y, Paz A, Sabo E, Potasman I. Fear of injections in young adults: Prevalence and associations. *Am. J. Trop. Med. Hyg* 2003;68:341–344. [PubMed: 12685642]
- [4]. Simonsen L, Kane A, Lloyd J, Zaffran M, Kane M. Unsafe injections in the developing world and transmission of blood-borne pathogens. *Bull. World Health Organ* 1999;77:789–800. [PubMed: 10593026]
- [5]. Miller MA, Pisani E. The cost of unsafe injections. *Bull. World Health Organ* 1999;77:808–811. [PubMed: 10593028]
- [6]. Toews DW. A communitywide needle/syringe disposal program. *Am. J. Public Health* 1995;85:1447–1448. [PubMed: 7573636]
- [7]. Prausnitz MR, Langer R. Transdermal drug delivery. *Nat. Biotechnol* 2008;26:1261–1268. [PubMed: 18997767]
- [8]. Mitragotri S, Blankschtein D, Langer R. Ultrasound-mediated transdermal protein delivery. *Science* 1995;269:850–853. [PubMed: 7638603]
- [9]. Wu XM, Todo H, Sugibayashi K. Effects of pretreatment of needle puncture and sandpaper abrasion on the in vitro skin permeation of fluorescein isothiocyanate (FITC)-dextran. *Int. J. Pharm* 2006;316:102–108. [PubMed: 16597490]
- [10]. Glenn GM, Flyer DC, Ellingsworth LR, Frech SA, Frerichs DM DM, Seid RC, Yu J. Transcutaneous immunization with heat-labile enterotoxin: development of a needle-free vaccine patch. *Expert Rev. Vaccines* 2007;6:809–819. [PubMed: 17931160]
- [11]. Banga AK. Microporation applications for enhancing drug delivery. *Expert Opin. Drug Deliv* 2009;6:343–354. [PubMed: 19348604]
- [12]. Daddona PE, Matriano JA, Mandema J, Maa Y-F. Parathyroid Hormone (1–34)-Coated Microneedle Patch System: Clinical Pharmacokinetics and Pharmacodynamics for Treatment of Osteoporosis. *Pharm. Res.* 2010 In Press.
- [13]. Zhu Q, Zarnitsyn VG, Ye L, Wen Z, Gao Y, Pan L, Skountzou I, Gill HS, Prausnitz MR, Yang C, Compans RW. Immunization by vaccine-coated microneedle arrays protects against lethal influenza virus challenge. *Proc. Natl. Acad. Sci* 2009;106:7968–7973.
- [14]. Kaushik S, Hord AH, Denson DD, McAllister DV, Smitra S, Allen MG, Prausnitz MR. Lack of pain associated with microfabricated microneedles. *Anesth. Analg* 2001;92:502–504. [PubMed: 11159258]
- [15]. Gill HS, Denson DD, Burris BA, Prausnitz MR. Effect of microneedle design on pain in human volunteers. *Clin. J. Pain* 2008;24:585–594. [PubMed: 18716497]
- [16]. Miyano T, Tobinga Y, Kanno T, Matsuzaki Y, Takeda H, Wakui M, Hanada K. Sugar micro needles as transdermic drug delivery system. *Biomed. Microdevices* 2005;7:185–188. [PubMed: 16133805]
- [17]. Ito Y, Yoshimitsu JI, Shiroyama K, Sugioka N, Takada K. Self-dissolving microneedles for the percutaneous absorption of EPO in mice. *J. Drug Target* 2006;14:255–261. [PubMed: 16882545]
- [18]. Sullivan SP, Murthy N, Prausnitz MR. Minimally invasive protein delivery with rapidly dissolving polymer microneedles. *Adv. Mater* 2008;20:933–938.

- [19]. Lee JW, Park JH, Prausnitz MR. Dissolving microneedles for transdermal drug delivery. *Biomaterials* 2007;29:2113–2124. [PubMed: 18261792]
- [20]. Chu LY, Choi S-O, Prausnitz MR. Fabrication of dissolving polymer microneedles for controlled drug encapsulation and delivery: Bubble and pedestal microneedle designs. *J. Pharm. Sci.* 2010 In Press.
- [21]. Choi SO, Rajaraman S, Yoon YK, Wu X, Allen MG. 3-D Metal patterned microstructure using inclined UV exposure and metal transfer micromolding technology. *Solid-State Sensor, Actuator, and Microsystems Workshop.* 2006
- [22]. Cormier M, Johnson B, Ameri M, Nyam K, Libiran L, Zhang DD, Daddona P. Transdermal delivery of desmopressin using a coated microneedle array patch system. *J. Control. Release* 2004;97:503–511. [PubMed: 15212882]
- [23]. Deacon B, Abramowitz J. Fear of needles and vasovagal reactions among phlebotomy patients. *J. Anxiety Disord* 2006;20:946–960. [PubMed: 16460906]
- [24]. Simonsen L, Clarke MJ, Schonberger LB, Arden NH, Cox NJ, Fukuda K. Pandemic versus epidemic influenza mortality: a pattern of changing age distribution. *J. Infect. Dis* 1998;178:53–60. [PubMed: 9652423]
- [25]. Prausnitz MR. Microneedles for transdermal drug delivery. *Adv. Drug Deliv. Rev* 2004;56:581–587. [PubMed: 15019747]
- [26]. Giudice EL, Campbell JD. Needle-free vaccine delivery. *Adv. Drug Deliv. Rev* 2006;58:68–89. [PubMed: 16564111]
- [27]. Arora A, Prausnitz MR, Mitragotri S. Micro-scale devices for transdermal drug delivery. *Inter. J. Pharm* 2008;364:227–236.
- [28]. McAllister DV, Wang PM, Davis SP, Park JH, Canatella PJ, Allen MG, Prausnitz MR. Microfabricated needles for transdermal delivery of macromolecules and nanoparticles: fabrication methods and transport studies. *Proc. Natl. Acad. Sci* 2003;100:13755–13760.
- [29]. Gill H, Prausnitz MR. Coated microneedles for transdermal delivery. *J. Control. Release* 2007;117:227–237. [PubMed: 17169459]
- [30]. Williams J, Fox-Leyva L, Christensen C, Fisher D, Schlichting E, Snowball M, Negus S, Mayers J, Koller R, Stout R. Hepatitis A vaccine administration: comparison between jet-injector and needle injection. *Vaccine* 2000;18:1939–1943. [PubMed: 10699344]

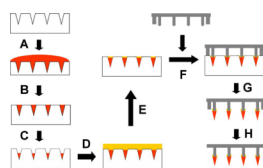


**Fig. 1.**

Schematic diagram of separable arrowhead microneedle fabrication process. (A) A drug solution was applied to a PDMS micromold under vacuum. (B) Excess drug solution on the mold surface was removed and saved for re-use. (C) The drug solution loaded in the mold cavities was dried under centrifugation. (D) A polymer solution was cast into the mold under vacuum. (E) Excess polymer solution on the mold surface was spun off by centrifugation. (F) Blunt metal shafts prepared by laser-cutting were aligned to the mold cavities. (G) The whole device was air-dried at room temperature or freeze-dried overnight. After drying, the dried, drug-filled polymer arrowheads connected to the metal shafts were removed from the mold. (H) Metal stoppers along the periphery of the patch were bent down.

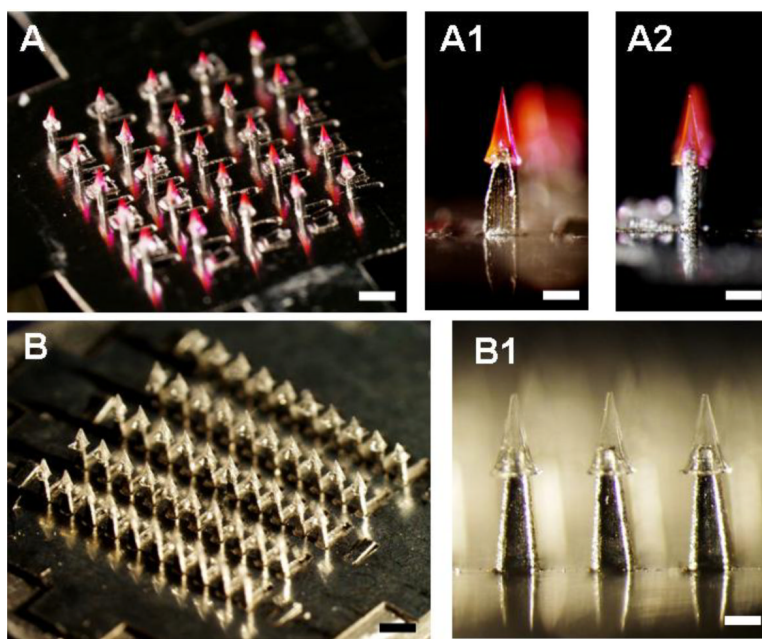


**Fig. 2.** Separable arrowhead microneedles. (A) A  $5 \times 5$  array of separable arrowhead microneedles comprising  $600 \mu\text{m}$ -tall metal shafts capped with  $600 \mu\text{m}$ -tall water-soluble PVA/PVP arrowheads encapsulating sulforhodamine. Bar =  $1 \text{ mm}$ . Individual needles are shown from the front (A1) and side (A2). Bar =  $300 \mu\text{m}$ . The red pyramidal structures are the arrowheads and the shiny structures below are the shafts. (B) A  $10 \times 5$  array of separable arrowhead microneedles comprising  $700 \mu\text{m}$ -tall metal shafts capped with  $600 \mu\text{m}$ -tall water-soluble PVA/sucrose arrowheads encapsulating inactivated influenza virus. Bar =  $1 \text{ mm}$ . A close up view shows individual needles under greater magnification (B1). Bar =  $300 \mu\text{m}$ .

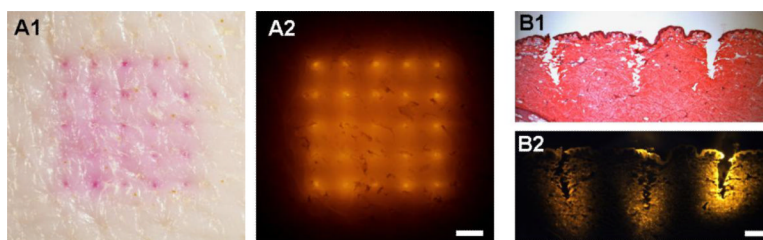


**Fig. 3.**

Insertion of separable arrowhead microneedles into porcine cadaver skin. En face view of skin imaged by brightfield (A1) and fluorescence (A2) optics after insertion and separation of sulforhodamine-loaded arrowheads from microneedles. Bar = 1 mm. The  $5 \times 5$  array of colored spots represent sulforhodamine encapsulated in arrowheads deposited in the skin. Histological cross section of a row of three microneedle insertion sites (B1) and the corresponding fluorescence image of sulforhodamine released from the arrowhead microneedles prior to H&E staining (B2). Bar = 300  $\mu\text{m}$ . The sites of microneedle insertion are seen by disruption of tissue structure (B1) and deposition of brightly colored sulforhodamine (B2). Microneedles had 600  $\mu\text{m}$ -tall shafts capped with 600  $\mu\text{m}$  tall PVP/PVA arrowheads encapsulating sulforhodamine.

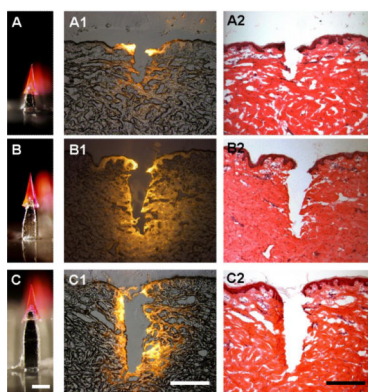


**Fig. 4.** The effect of microneedle shaft length on arrowhead insertion depth into porcine cadaver skin. Arrowheads measuring 600  $\mu\text{m}$  tall and encapsulating sulforhodamine mounted on shafts measuring 300  $\mu\text{m}$  (A), 600  $\mu\text{m}$  (B) and 900  $\mu\text{m}$  (C) were inserted into skin, which was imaged after histological sectioning by fluorescence microscopy (A1, B1, C1) and H&E staining (A2, B2, C2). Bar = 300  $\mu\text{m}$

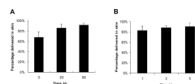


**Fig. 5.**

Delivery efficiency of sulforhodamine in porcine cadaver skin using separable arrowhead microneedles. The percentage of encapsulated sulforhodamine released into the skin is shown as a function of time after microneedle insertion into the skin without mechanical perturbation (A) and with arrowhead separation facilitated by manual vibration for  $< 1$  s (B). Microneedles had  $600\ \mu\text{m}$ -tall shafts capped with  $600\ \mu\text{m}$  tall PVP/PVA arrowheads encapsulating sulforhodamine. Data represent the mean value of four replicate measurements  $\pm$  standard deviation.



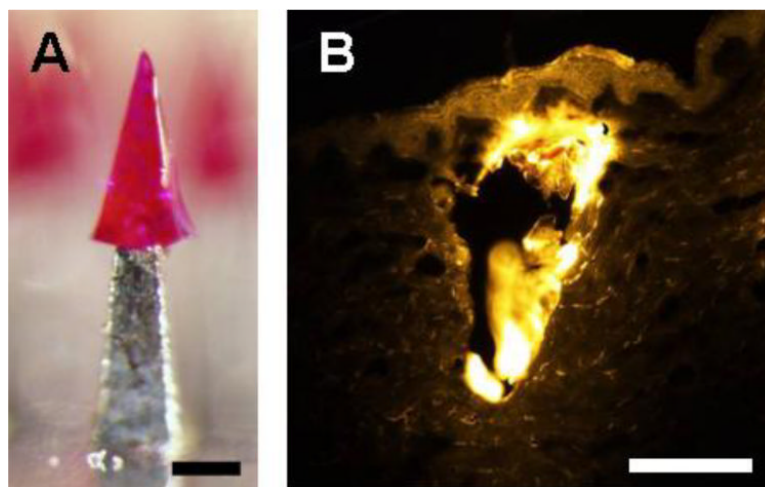


**Fig. 6.** Deposition of biodegradable PLGA arrowhead in porcine cadaver skin. (A) A 600  $\mu\text{m}$ -tall arrowhead made of PLGA encapsulating sulforhodamine capped onto a 600  $\mu\text{m}$ -tall shaft. (B) Histological section of a PLGA arrowhead deposited within skin imaged by fluorescence microscopy. The bright yellow portion of the image shows the arrowhead surrounded by weakly fluorescent skin tissue. The microneedle was inserted into the skin for 1 s and was vibrated to allow immediate separation from the shaft. Bars = 200  $\mu\text{m}$ .

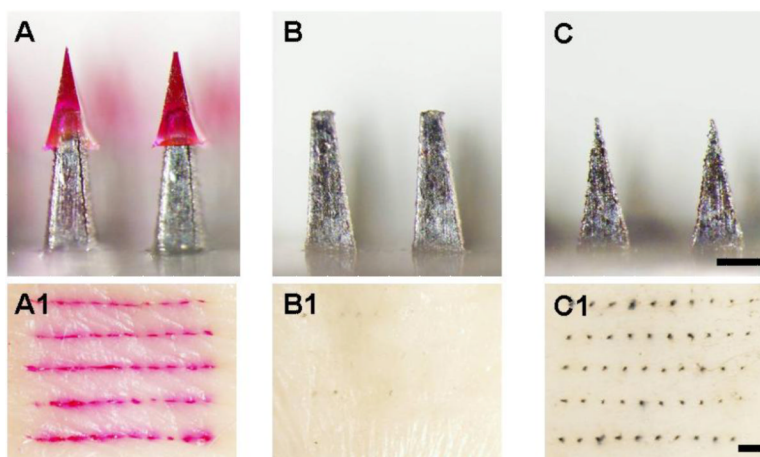


**Fig. 7.**

Evaluation of microneedle safety after arrowhead separation. Microneedle devices (A, B, C) were inserted into human cadaver skin and assayed for microneedle penetration into the skin by brightfield microscopy (A1, B1, C1). (A) Microneedles comprising a 600  $\mu\text{m}$ -tall arrowhead encapsulating sulforhodamine capping a 700  $\mu\text{m}$ -tall shaft with approximately 200  $\mu\text{m}$  overlap between the arrowhead and the shaft. After insertion into skin, the array of sulforhodamine-encapsulating arrowheads is evident in the skin (A1). (B) Blunt 700  $\mu\text{m}$ -tall microneedle shafts that represent separable arrowhead microneedles after arrowhead separation. These blunt shafts were not able to penetrate into skin, as shown by a lack of staining with tissue marking dye (B1). (C) Sharpened 700  $\mu\text{m}$ -tall microneedle shafts with the same height and base width as in (B). These sharp-tipped structures easily penetrated skin, as shown by staining with dye (C1). Top Row: Bar = 300  $\mu\text{m}$ ; Bottom Row: Bar = 1 mm.